XXVII Brazilian Congress in Biomedical Engineering

October 26-30 2020 Vitoria (Brazil)

Preface

For this edition of the Brazilian Conference on Biomedical Engineering (CBEB2020 – Congresso Brasileiro de Engenharia Biomédica), 665 papers were submitted, composed of 564 scientific articles (4-6 pages) and 101 Scientific Communications (Abstracts up to 2 pages). After the first round of reviews, 595 papers were accepted (514 full papers and 81 scientific communication). These 595 articles underwent a second review round, and at the end 551 papers (478 full papers and 73 scientific papers) were accepted to be presented at CBEB2020.

CBEB is promoted by the Brazilian Society of Biomedical Engineering (SBEB), with biannual periodicity, organized by researchers linked to a local research institution, with the collaboration of the entire scientific community linked to the area of Biomedical Engineering in Brazil. CBEB2020 was held on October 26-30, 2020 in Vitória (Brazil) and was organized in the following tracks:

- Clinical Engineering and Health Technology Assessment
- Biomaterials
- Tissue Engineering and Artificial Organs
- Bioengineering
- Biomedical Devices and Instrumentation
- Biomechanics and Rehabilitation
- Neuroengineering
- Biomedical Signal and Image Processing
- Biomedical Robotics, Assistive Technologies, and Health Informatics
- Biomedical Optics and Systems and Technologies for Therapy and Diagnosis
- Basic Industrial Technology in Health
- Special Topics

We would like to thank the sponsors CNPq and FAPES for making it possible to celebrate this event in times of uncertainty due to the COVID-19 pandemics.

October 26-30, 2020
Vitória - Brazil

Teodiano Bastos-Filho
Anselmo Frizera-Neto
Eliete Maria de Oliveira Caldeira

Proposal of a Low Profile Piezoelectric Based Insole to Measure the Perpendicular Force Applied by a Cyclist

M.O. Araújo[1] and A. Balbinot[1]

[1] UFRGS/PPGEE, Laboratory of Electro-Electronic Instrumentation (IEE), Porto Alegre, Brazil

Abstract— **This paper presents the development of a one-dimensional force platform for the pedaling analysis in a bicycle using piezoelectric films. A 3D-printed insole was designed to accommodate an array of Polyvinylidene Fluoride films without changing the pedaling characteristic. The sensor's positioning sought to cover the point of contact between the shoe and the pedal. An instrumentation amplifier, a charge amplifier and an anti-aliasing filter with a cutoff frequency of 20Hz composed the conditioning circuit. The system dynamic calibration was executed with the application of mechanical impulses to the sensors' surface using an impact hammer of model 8206 by Brüel&Kjær, and a chassis model NI SCXI-1600 acquired the output signal. Hence, the experimental transfer functions were defined for each one of the 20 channels of the system. The maximum linearity error was 5.98% for the channel #4 of the right insole and 5.81% for the channel #7 of the left insole. A NI USB-6289 board acquired the data coming from the trials with a bicycle. In the collected data analysis, it was possible to define the pedaling phases by observing the sum of all channels for each insole. The average value for the maximum force applied on the right insole was 235.8N, and the average value for the maximum force applied on the left insole was 223.2N. It was possible to map the zones of greater and minor activation during the movement via a single channel analysis for each insole, being the regions of greatest activation located at the top of the medial forefoot region (right foot), and at the bottom of the lateral forefoot region (left side). The regions with the least activation are at the bottom of the medial forefoot region (at the end of the medial longitudinal arch) on both sides.**

Keywords— **force platform, one-dimensional, pedaling force, piezoelectric films, insole.**

I. Introduction

Cycling is, beyond any doubt, one of the most widespread and worshiped sports around the world. Whether for recreation or performance purposes, the bicycle tends to become part of our lives due to its eco-friendly character, replacing traditional motor vehicles. As a result, a large number of publications have been made, such as [1], on new experimental discoveries on the biomechanics of cycling, to know with scientific rigor the relations of forces applied in the act of pedaling [2].

The growing demand concerning performance sports drives the need for measures increasingly closer to the point of contact between athletes and equipment. The efficiency of the pedaling force in cycling is usually measured by the relationship between the force perpendicular to the crank, and the total force applied to the pedal [3].

To carry out such force measurements, the precise characterization of the mechanical loads imposed on the pedal represents a fundamental element [4]. The challenge is to implement the measurements in the least invasive way, preserving the ergonomics and the original geometry of the structure to the maximum. This objective is achieved, for example, with the use of pressure-sensitive membranes or films. In the case presented here, the choice is piezoelectric polymeric films - specifically, PVDF (Polyvinylidene Fluoride) films [5].

Historically, force measurements on pedals are performed using strain gauges [6, 7, 1]. However, the distribution of strain gauges reportedly presents significant cross-sensitivity [4]. The moment application in one of the axis generates strain in the remainder of the axes, which makes the system calibration complex and expensive. To eliminate cross-sensitivity issues, the use of multi-directional piezoelectric sensors was studied. Works have been proposed, such as Ericson & Nisell [8] and Broker & Gregor [4], looking for the use of commercially available sensors in pedal instrumentation.

Hence, the present work sought to measure the force directly at its point of application. Generally, this measurement occurs via pedal or crank arm instrumentation. In this context, the main objective is to build a one-dimensional force platform in the shape of an insole instrumented with PVDF films with the purpose of measuring the force exerted during the act of pedaling. With an acquisition and storage system, data analysis took place to prove its usefulness in the area.

Throughout the development, the miniaturization of the system and the maintenance of non-invasiveness of the method, to preserve the naturalness of the movements. Therefore, we sought to expand the concept of an instrumented pedal, minimizing the profile and valuing the point of contact between foot and pedal. For such, the proposed instrumented insole replaced the structure already present in the shoe with-

out adding volume - which preserves comfort and maximizes movement fidelity. With a competitive appeal, SPD (Shimano Pedalling Dynamics) was used, one of the most widespread in a high-performance environment. It is worth noting that this is a one-dimensional analysis of the applied effort, which means that it only covers the vertical force.

II. Materials and Methods

A. 3D-Printed Insole Sctructure

The commercial cycling shoes used (SH-M065L, from Shimano) has a sole and midsole presented in one piece. However, unlike ordinary shoes in which the midsole is a smooth structure, this shoe has recesses that prevent the direct cementation of sensors in the region where the force is applied. At the same time, the original insole is very soft, favoring the deflection of the sensors. Also, it does not offer the possibility of using wires without physical interference in the activation of the sensors. Thus, the design of a new insole proved to be necessary.

The development began by identifying the desirable requirements for the new insole. To address the limitations of the original structure, these are the characteristics of the so considered ideal solution:

- dimensions compatible with the original insole;
- uniform and solid surface in the cementation region;
- flexibility of the structure as a whole;
- passageways for wiring.

Using the SolidWorks 2012 software, the design considered the highest possible level of ergonomics, i.e., it followed the original insole's organic lines. The material of choice was TPU (thermoplastic polyurethane), which has elasticity as main characteristic [9]. However, in a multi-layer arrangement, the structure becomes stiff to well distributed compression. A solid extrusion serves as a platform at the point of application of force to generate full support for the sensors. It prevents their deflection - an action that may affect the readings. Also, a hexagonal pattern applied to the remainder of the insole provides mechanical strength and levels the rest of the structure with the cementation region. The structure is seen in Figure 1 along with its dimensions and sensor positioning.

As a result, the insoles offer rigidity for the sensors and flexibility for handling. It is worth mentioning that the deflection of the sensors remains undesirable. However, as the shape of the piece follows the outline of the midsole, no movement is expected during pedaling.

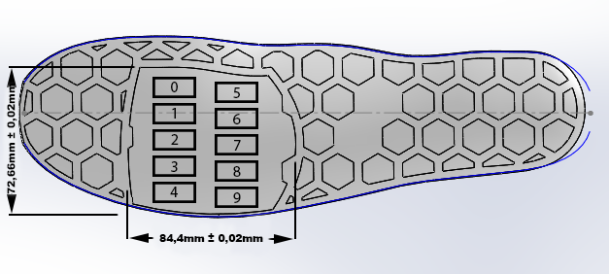

Fig. 1: Insole (left foot) with solid extrusion and passageways for wiring and sensor positioning

B. Piezoelectric film array

The role of the piezoelectric film array is to translate mechanical stress into electrical signal. To obtain the largest measurable area of interest for the insole, the sensor of choice was the smallest commercially available film from the manufacturer MSI (Measurement Specialties, Inc.): the LDT0-028K [10]. Its active surface corresponds to $153mm^2$, which allows the placement of 10 distinct films in the area of interest. This made it possible to execute a more in-depth study of the pedaling cycle.

Piezoelectric films have a set of mechanical and electrical characteristics that shape its signal output. For forces applied perpendicularly to the sensor, the key parameter is the piezo strain constant d_{33} [11], which is determined by the reason between charge ($Q[C]$) and applied force ($F[N]$). The Equation 1 describes the relationship between these variables.

$$d_{33} = \frac{Q}{F}\left[\frac{C}{N}\right] \tag{1}$$

The conditioning circuit of choice is composed of: an instrumentation amplifier, mainly to reduce common mode noise and to apply gain without adding offset with gain of approximately 32; a charge amplifier with gain of approximately 10^7, approaching the piezoelectric film as a charge pump; and an anti-aliasing filter, a low-pass Sallen Key with cutoff frequency of $20Hz$. Hence, the output signal, proportional to the force applied to a single sensor, is given by Equation 2.

$$V_{Output} = 4.488 \cdot 10^{-3} F[V] \tag{2}$$

C. Calibration procedure

The dynamic calibration procedure consisted of applying a series of mechanical impulses to the piezoelectric films, acquiring, in a synchronous manner, the responses of the impact hammer and each one of the 20 channels. According to

[12], the Type 8206 impact hammer has known sensibility of $23.91[mV/N]$. Thus, considering Equation 1, it was possible to determine the transfer function for every placed sensor. The calibration of piezoelectric films is a challenge due to the equipment. The best way to do it would be having a high speed hydraulic press or a customized device to apply even pressure on the sensor, which unfortunately wasn't available to the project. That said, the use of an impact hammer is acceptable, but not optimal.

The calibration equipment used to gather data was composed of a NI SCXI-1600 [13] chassis and a SCXI-1530 [14] accelerometry module for the impact hammer, and a NI USB-6289 DAQ [15] for the 20 channels from the insoles. All channels were acquired at a $1kHz$ rate. The integration has been made using LabVIEW^{TM} 2013, in which a routine took care of acquiring and synchronizing data from the sources.

D. Trials

Volunteers were asked to wear the system (Figure 2), placing the conditioning circuits around their ankles and carefully put on the shoes. Information on volunteers may be found in Table 1. All 5 volunteers have the same shoe size (41 BR).

Table 1: Information on volunteers

Volunteer	Body mass $[kg]$	Height $[m]$	Dominant leg
1	81	1.87	Right
2	70	1.77	Right
3	71	1.89	Right
4	66	1.81	Right
5	67	1.74	Right

The tests occurred as follows: the volunteer had ten rounds of acquisitions with 60 seconds each, aiming at a medium cadence movement (around $1Hz$) starting from rest. A software interface was created via LabVIEW^{TM} 2013, with a well-defined sequence of steps:

1. Start of the program (15 seconds of no action to position the volunteer / start of the medium cadence movement);
2. Sequence of audible signals indicating the beginning of acquisitions;
3. Cadence starts from rest.

It is worth remembering that, in the case of inexperienced volunteers concerning the clipless pedals, preliminary tests made sure that the volunteer could acquaint the clipping movement. The protocol is in accordance with the Declaration of Helsinki of the World Medical Association, as the subjects have declared consent in participating. The Institutional Review Board of the Federal University of Rio Grande do Sul approved this study under the Certificate of Presentation for Ethical Appreciation (CAAE) number: 11253312.8.0000.5347.

Fig. 2: Cycling shoes with instrumented insoles and conditioning circuits

III. Results

A. Dynamic Calibration

Following the guidelines described in Section C., the transfer functions for each one of the piezoelectric films were determined (Tables 2 and 3).

Table 2: Transfer functions (TF), sensitivity (S) and linearity error (ε_{lin}) for the right foot

Channel	$TF\ [V]$	$S\ [V/N]$	ε_{lin}
0	$4.39 \cdot 10^{-3}F - 0.0057$	$4.39 \cdot 10^{-3}$	4.48%
1	$4.56 \cdot 10^{-3}F - 0.0344$	$4.56 \cdot 10^{-3}$	5.78%
2	$4.82 \cdot 10^{-3}F - 0.0008$	$4.82 \cdot 10^{-3}$	3.98%
3	$4.51 \cdot 10^{-3}F - 0.0302$	$4.51 \cdot 10^{-3}$	4.83%
4	$4.55 \cdot 10^{-3}F + 0.0076$	$4.55 \cdot 10^{-3}$	5.98%
5	$4.11 \cdot 10^{-3}F - 0.0262$	$4.11 \cdot 10^{-3}$	5.41%
6	$4.29 \cdot 10^{-3}F - 0.0019$	$4.29 \cdot 10^{-3}$	3.87%
7	$4.38 \cdot 10^{-3}F - 0.0898$	$4.38 \cdot 10^{-3}$	5.89%
8	$4.41 \cdot 10^{-3}F - 0.0452$	$4.41 \cdot 10^{-3}$	5.67%
9	$4.78 \cdot 10^{-3}F + 0.0068$	$4.78 \cdot 10^{-3}$	4.91%

Table 3: Transfer functions (TF), sensitivity (S) and linearity error (ε_{lin}) for the left foot

Channel	$TF\ [V]$	$S\ [V/N]$	ε_{lin}
0	$5.08 \cdot 10^{-3}F - 0.0110$	$5.08 \cdot 10^{-3}$	2.69%
1	$4.31 \cdot 10^{-3}F + 0.0138$	$4.31 \cdot 10^{-3}$	4.84%
2	$4.85 \cdot 10^{-3}F - 0.0441$	$4.85 \cdot 10^{-3}$	2.98%
3	$4.70 \cdot 10^{-3}F - 0.0794$	$4.70 \cdot 10^{-3}$	5.16%
4	$4.90 \cdot 10^{-3}F + 0.0419$	$4.90 \cdot 10^{-3}$	4.89%
5	$4.34 \cdot 10^{-3}F + 0.0321$	$4.34 \cdot 10^{-3}$	4.11%
6	$4.44 \cdot 10^{-3}F + 0.0546$	$4.44 \cdot 10^{-3}$	4.13%
7	$4.34 \cdot 10^{-3}F + 0.0723$	$4.34 \cdot 10^{-3}$	5.81%
8	$4.13 \cdot 10^{-3}F - 0.0720$	$4.13 \cdot 10^{-3}$	4.43%
9	$4.24 \cdot 10^{-3}F - 0.0319$	$4.24 \cdot 10^{-3}$	5.47%

B. *Waveform during trials*

The group of volunteers performed a set of trials as described in Section D.. Figure 3 shows a 5 seconds extract of acquisition for both feet for individual #1. All the channels for a foot were combined into one signal, representing the total force exerted by the volunteer. The option for this type of visualization avoids information clutter due to showing 10 channels at once for each foot. The data from this graph will be unwrapped in Section IV.

Results considering the average value of peak forces applied by the volunteers may be seen in Table 4. Concerning this data, the mean value for the applied force was 235.8N with a standard deviation of 25.7N on the right foot, and 223.16N with a standard deviation of 25.0N on the left foot.

Table 4: Peak forces (sum) applied by each volunteer

Side	I1	I2	I3	I4	I5
R	212.8N	252.4N	275.8N	206.2N	231.8N
L	192.7N	245.3N	242.9N	192.5N	242.4N

Table 5 shows the average value for peak forces during the trials considering individual channels. Values in bold font represent the maximum value for a volunteer, while values in italic represent the minimum values for a volunteer. Figure 4 shows a heatmap representing the average value for peak forces considering volunteer #2.

Table 5: Average force (maximum value) applied for each channel and each individual

Ch.	Side	I 1	I 2	I 3	I 4	I 5
0	R	35.3N	**48.6N**	**40.0N**	24.16N	**53.4N**
	L	30.5N	33.9N	30.0N	32.31N	44.4N
1	R	31.3N	37.3N	31.19N	41.3N	24.1N
	L	26.7N	29.4N	23.8N	22.8N	33.6N
2	R	24.9N	23.1N	26.3N	21.2N	21.2N
	L	23.5N	34.2N	31.9N	29.5N	29.1N
3	R	24.5N	24.5N	27.6N	*15.9N*	24.9N
	L	21.3N	29.4N	27.3N	25.5N	25.0N
4	R	**38.7N**	45.6N	39.8N	30.4N	41.6N
	L	25.2N	35.7N	27.5N	33.1N	30.6N
5	R	21.4N	31.9N	28.2N	**41.7N**	21.0N
	L	15.7N	16.9N	*12.4N*	*8.5N*	28.3N
6	R	*13.1N*	*14.7N*	30.7N	25.7N	*13.1N*
	L	*9.5N*	*12.6N*	13.8N	15.5N	*16.1N*
8	R	19.5N	17.2N	*16.3N*	23.6N	31.8N
	L	20.4N	26.5N	29.2N	18.5N	39.7N
9	R	37.0N	43.9N	24.9N	37.4N	46.8N
	L	**38.0N**	**43.0N**	30.9N	**38.3N**	**49.8N**

IV. Discussion

It is noticeable that the linearity error for the calibration procedure is below 5% (or around this value). The average sensitivity is $4.51 \cdot 10^{-3}V/N$ with a standard deviation of $0.27 \cdot 10^{-3}V/N$. Considering the standard uncertainty calculated for the system's output sensitivity ($\pm 3.67 \cdot 10^{-4}V/N$), channel 5 of the right insole and channels 0 and 4 of the left insole are outside the stipulated limit range ($[4.121 \cdot 10^{-3}V/N; 4.855 \cdot 10^{-3}V/N]$).

The hypothesis is that this occurs because the response characteristic undergoes significant changes due to the curves of the insole, since the films are in a permanent state of flexion. Also, the insole surface is not entirely smooth: the 3D construction presents a step of 0.1 mm between one layer and another, contributing to the total non-cementation of the film and a small deflection in the region during the application of effort (which can also modify the response of the film).

Observing Figure 3, the anti-symmetry of the acquired signals is clear, which is a coherent result knowing that each leg exerts an effort in approximately half of the pedaling cycle [2] in counter-phase. According to data, it's noticeable that the volunteers have difficulty in completely removing the force applied during the recovery phase, especially regarding the non-dominant leg. This behavior appoints the several retakes of force application during this phase, prominent in the negative part of the acquired signals. The phenomenon increases the requirement of the limb that is in the propulsion phase, culminating in the eventual waste of energy. As well, although Table 5 shows that the dominant limb presented greater activation in most cases, Figure 3 shows that subject #2 presented greater force in the non-dominant limb (at least in the excerpt). One of the factors to which the phenomenon can be attributed is the adaptation of the subjects to

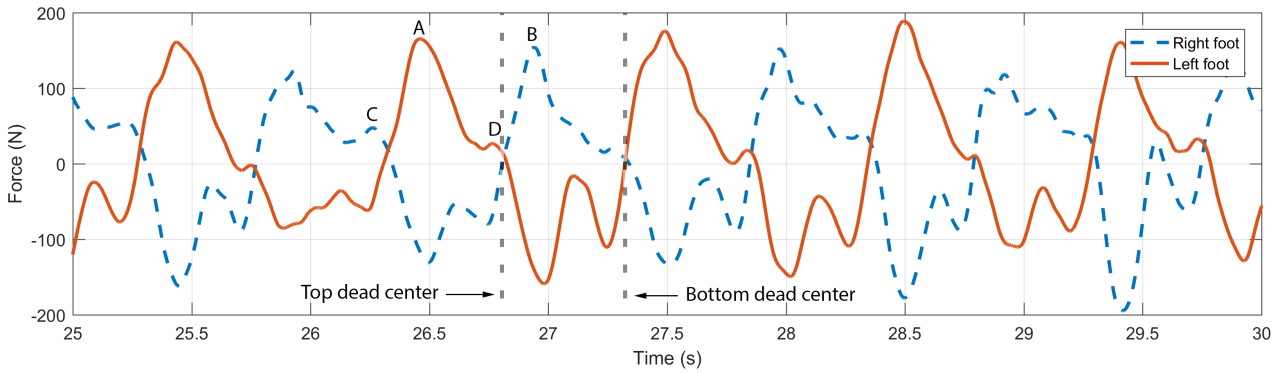

Fig. 3: Extract of an acquisition by volunteer #1 (sum of all channels for each foot). A and B: Points of maximum power for the cycle (right and left sides, respectively; C and D: Second point of application of force (righ and left sides, respectively)

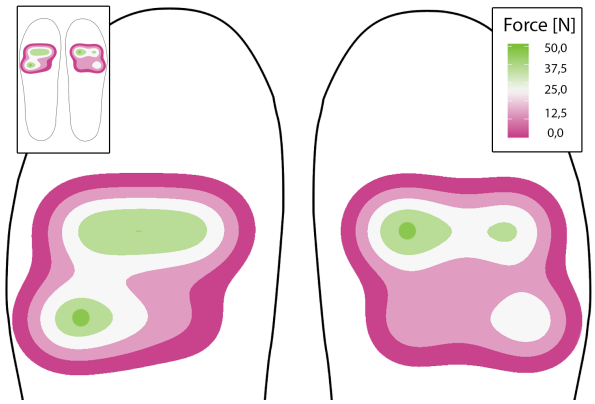

Fig. 4: Heatmap for the average value for peak forces during the trials (volunteer #2)

the bicycle as a whole, generating a variation due to fit inconsistencies and ends up creating this behavior.

Note that, immediately after the top dead center, the application of force is initiated. After reaching the peak of force application (at approximately 90^o), there is still a second point of force application before reaching the bottom dead center, where the recovery phase begins and the application of force is practically stopped, occurring an opposite signal peak indicating the withdrawal of force applied to the sensor.

Concerning the sensor activation (see Table 5), it is noted that the regions of greatest activation are located near sensor #0 (ball of the foot) to the right side, and close to sensor #9 (encounter of the previous transverse arch and the lateral longitudinal arch) to the left side. The regions with the least activation are located near sensors #5 and #6 (medial longitudinal arch) on both sides. It gives a hint that individuals tend to use the outer part of the non-predominant limb (supination) while pedaling. Also, it is worth remembering that despite the foot retention system, the shoe cleat allows a limited degree of freedom (6^o). Furthermore, an additional degree of freedom for movement inside the shoe may cause effort deviation in favor of lateral forces. Unfortunately, it's not a measurable variable since the developed insole takes only the perpendicular force into account. To address this issue, a new 6 degree of freedom system is being developed, rendering it possible to quantify the effect of the aforementioned variables.

When Table 5 is, again, observed, it's noticed that the activation pattern is slightly different for each individual. This behavior is attributed to the bicycle assembly, which can play a considerable role in the activation pattern, since the adjustment of the parts contribute to the biomechanics of the movement and, consequently, to the effectiveness and better use of efforts (saddle and seatpost [16], for instance) . Besides, each subject has a different plantar structure, contributing so that the pressure distribution is not the same for everyone.

V. Conclusions

In this project, we sought to develop a non-invasive force platform capable of measuring the pedaling force without changing the movement ergonomics. Thus, a study was conducted on the behavior of the piezoelectric films of choice for the movement of interest, seeking the development of the entire conditioning chain to maximize the response for the best possible signal acquisition. All stages of the project were validated with the aid of gauged instruments, with a maximum linearity error of 5.98%.

The proposed set of trials revealed that piezoelectric films are capable of transcribing the nuances of the pedaling movement, making it possible to study its state on different phases. Also, such results prove that, despite the dynamic nature of piezoelectric films, it is possible to use them to measure low-

frequency phenomena and to map the pedal movement.

Therefore, the present work proves the viability of a system composed of piezoelectric films for the measurement and the mapping of the pedaling force. However, for the system to evolve to such an extent, it is necessary to carry out more tests (and with more volunteers). Also, modifying the calibration procedure and the insole construction to avoid the reported issues is crucial to take the concept to a higher level. That being the case, it will be possible to consolidate the system as a tool for pedal force analysis, being used, for instance, to determine the profile needed for a padding insole to enhance effort distribution.

Conflict of Interest

The authors declare that they have no conflict of interest.

Acknowledgements

The present work was financially supported by the Conselho Nacional de Desenvolvimento Científico e Tecnológico (CNPq) - grants no. 136036/2019-8 - and was financed in part by the Coordenação de Aperfeiçoamento de Pessoal de Nível Superior - Brasil (CAPES) - Finance Code 001.

References

1. Pigatto Andre V., Moura Karina O.A., Favieiro Gabriela W., Balbinot Alexandre. A new crank arm based load cell, with built-in conditioning circuit and strain gages, to measure the components of the force applied by a cyclist in *Proceedings of the Annual International Conference of the IEEE Engineering in Medicine and Biology Society, EMBS*;2016-Octob:1983–1986 2016.
2. Bini R.R., Carpes F.P.. *Biomechanics of Cycling*. Springer International Publishing 2014.
3. Bini R.R., Hume P.A., Croft J., Kilding A.R.. Pedal force effectiveness in Cycling: a review of constraints and training effects *Journal of Science and Cycling.* 2013;2:11–24.
4. Broker Jeffrey P., Gregor Robert J.. A Dual Piezoelectric Element Force Pedal for Kinetic Analysis of Cycling *International Journal of Sport Biomechanics.* 1990;6 DOI:10.1123/ijsb.6.4.394.
5. Kawai Heiji. The Piezoelectricity of Poly (vinylidene Fluoride) *Japanese Journal of Applied Physics.* 1969;8 DOI:10.1143/jjap.8.975.
6. Davis R.R., Hull M.L.. Measurement of pedal loading in bicycling *Journal of Biomechanics.* 1981;14 DOI:10.1016/0021-9290(81)90145-7.
7. Lazzari Caetano Decian, Balbinot Alexandre. S e n s o r s & T r a n s d u c e r s Wireless Crankarm Dynamometer for Cycling 2011;128:39–54.
8. Ericson M. O., Nisell R.. Efficiency of pedal forces during ergometer cycling *International Journal of Sports Medicine.* 1988;9 DOI:10.1055/s-2007-1024991.
9. ACC . Introduction to Polyurethanes: Thermoplastic Polyurethane 2012. Available at https://polyurethane.americanchemistry.com/polyurethanes/Introduction-to-Polyurethanes/Applications/Thermoplastic-Polyurethane/.
10. Measurement Specialties Inc. . *LDT with Crimps Vibration Sensor/Switch* 2017. Available at https://cdn.sparkfun.com/datasheets/Sensors/ForceFlex/LDT{_}Series.pdf.
11. Measurement Specialties Inc. . *Piezo Film Sensors* 1999. Available at https://mma.pages.tufts.edu/emid/piezo.pdf.
12. Brüel&Kjær . *Type 8206 Product Data*. Brüel&Kjær 2016. Available at https://www.bksv.com/-/media/literature/Product-Data/bp2078.ashx.
13. National Instruments . *SCXI-1600 User Manual* 2004. Available at https://www.ni.com/pdf/manuals/373364c.pdf.
14. National Instruments . *SCXI-1530/1531 User Manual* 2000. Available at https://www.ni.com/pdf/manuals/322642a.pdf.
15. National Instruments . *NI 6289* 2016. Available at https://www.ni.com/pdf/manuals/375222c.pdf.
16. Bini Rodrigo R., Hume Patria A., Crofta James L.. Effects of saddle height on pedal force effectiveness *Procedia Engineering.* 2011;13 DOI:10.1016/j.proeng.2011.05.050.

Authors: Matheus de Oliveira Araújo and Alexandre Balbinot
Institute: Federal University of Rio Grande do Sul
Street: Av. Osvaldo Aranha, 103 - 206D
City: Porto Alegre
Country: Brazil
Email: mdeoliveira.araujo@gmail.com and abalbinot@gmail.com